ACS APPLIED MATERIALS & INTERFACES

Research Article

Cite This: ACS Appl. Mater. Interfaces 2018, 10, 39228−39237

www.acsami.org

Heterostructured Silk-Nanofiber-Reduced Graphene Oxide Composite Scaffold for SH-SY5Y Cell Alignment and Differentiation

Huaibin Qing,[†,‡,#,○] Guorui Jin,[‡,▽,○] Guoxu Zhao,[‡,▽] Guoyou Huang,[‡,▽] Yufei Ma,[‡,▽] Xiaohui Zhang,[‡,▽] Baoyong Sha,[‡,⊥] Zhengtang Luo,[∥] Tian Jian Lu,[#,▽,△,*] and Feng Xu[‡,▽,*]

[†]State Key Laboratory for Mechanical Behavior of Materials, Xi'an Jiaotong University, Xi'an 710049, P.R. China

[‡]The Key Laboratory of Biomedical Information Engineering of Ministry of Education, Xi'an Jiaotong University, Xi'an 710049, P.R. China

[#]State Key Laboratory of Mechanics and Control of Mechanical Structures, Nanjing University of Aeronautics and Astronautics, Nanjing 210016, P.R. China

[▽]Bioinspired Engineering and Biomechanics Center (BEBC), Xi'an Jiaotong University, Xi'an 710049, P.R. China

[⊥]Institute of Basic Medical Science, School of Basic Medical Science, Xi'an Medical University, Xi'an 710021, China

[∥]Department of Chemical and Biomolecular Engineering, The Hong Kong University of Science and Technology, Clear Water Bay, Kowloon, Hong Kong

[△]MOE Key Laboratory for Multifunctional Materials and Structures, Xi'an Jiaotong University, Xi'an 710049, P.R. China

Supporting Information

ABSTRACT: Stem cell therapy is promising for treating traumatic injuries of the central nervous system, where a major challenge is to effectively differentiate neural stem cells into neurons with uniaxial alignment. Recently, controlling stem cell fate by modulating biophysical cues (e.g., stiffness, conductivity, and patterns) has emerged as an attractive approach. Herein, we report a new heterostructure composite scaffold to induce cell-oriented growth and enhance the neuronal differentiation of SH-SY5Y cells. The scaffold is composed of aligned electrospinning silk nanofibers coated on reduced graphene paper with high conductivity and good biocompatibility. Our experimental results demonstrate that the composite scaffold can effectively induce the oriented growth and enhance neuronal differentiation of SH-SY5Y cells. Our study develops a novel scaffold for enhancing the differentiation of SH-SY5Y cells into neurons, which holds great potential in the treatment of neurological diseases and injuries.

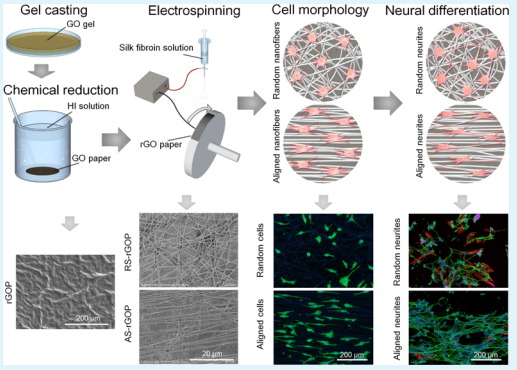

KEYWORDS: *graphene oxide, silk nanofibers, electrospinning, stem cell, tissue engineering, cell microenvironment*

1. INTRODUCTION

Lots of people worldwide suffer from the central nervous system injuries, including traumatic brain injury and spinal cord injury, as well as neurological diseases such as Alzheimer's disease, Parkinson's disease, and Huntington's disease.[1] Treatment of neurological diseases or injuries is challenging because of the limited regeneration capability of central neurons.[2] Stem cell therapy is emerging as a promising strategy for neural repair and regeneration. Among various stem cells, neural stem cells (NSCs), which are multipotent with the ability to differentiate into neurons and secrete multiple neurotrophic factors via paracrine activity, show great potential for neural regeneration.[3,4] Many studies have proved that the differentiated NSCs with high neural protein expression, extended neurite length and alignment, and neuron functionalities are highly desired for effective regeneration of neural tissues.[5−7]

To date, various biochemical cues (e.g., retinoic acid (RA), valproic acid, and oleanolic acid) have been intensively used to induce differentiation of NSCs into neurons.[8−10] However, most NSCs differentiate more likely toward glial cells than neurons with only biochemical cues.[11] Recently, accumulating evidence has shown that biophysical cues (e.g., electrical stimulation[12−14] and nanotopographical features[15]) have also shown significant capability in promoting the neuronal differentiation of NSCs.[16] Various conductive and biocompatible materials have been developed for providing electrical stimulation to cells (e.g., polyaniline and polypyrrole).[17,18] Among these, graphene-based materials have attracted special attention because of their extraordinary electrical conductivity,[19] excellent mechanical stability,[20] and favorable biocom-

Received: July 25, 2018
Accepted: September 18, 2018
Published: September 18, 2018

DOI: 10.1021/acsami.8b12562
ACS Appl. Mater. Interfaces 2018, 10, 39228−39237

patibility.[6] Graphene materials have been proved to effectively enhance the neuronal differentiation of NSCs, promote the neurite sprouting and outgrowth, and improve neural activity upon electrical stimulation.[6,11,21,22] However, the differentiated neurons on the graphene films usually have random alignment, limiting the formation of interconnected neural networks.[21,23]

To address this issue, nanofibrous scaffolds made of natural polymers such as collagen, gelatin, fibrin, and silk have been used to extend neurites.[24−26] Among these natural proteins, silk fibroin has drawn significant attention because of its biocompatibility, biodegradability, and superior performances.[27] Importantly, silk nanofibrous scaffolds are considered ideal for nerve cell culture because of the programmable nanotopographical structure mimicking the native extracellular matrix (ECM) for cell attachment and proliferation.[28,29] For instance, aligned silk (AS) fibrous scaffolds have been shown to support the culture of NSCs, stimulate the neurite outgrowth, and promote the neurite extension.[30] However, the neuronal differentiation of NSCs on such nonconductive nanofibrous scaffolds is still suboptimal.[31] Therefore, there is still an unmet need for a new scaffold with good biocompatibility, conductivity, and aligned nanotopographical feature, which can effectively induce the differentiation of NSCs toward neurons with high protein expression, guided neurite alignment, and well-formed neural network.

In this work, we developed a new heterostructured composite scaffold composed of aligned electrospinning silk nanofibers coated on conductive reduced graphene paper (rGOP) to enhance the neuronal differentiation of SH-SY5Y cells, in terms of neural protein expression, neurite extension and alignment, and neural network formation. We first examined the surface features and conductivity of the silk-nanofiber-coated rGOP heterogeneous composite scaffold. We further studied the adhesion, morphology, proliferation, and neuronal differentiation of SH-SY5Y cells seeded onto the scaffolds. Our study develops a novel scaffold for enhancing the differentiation of SH-SY5Y cells into neurons on the silk nanofiber−rGOP, which holds great potential in the treatment of neurological diseases and injuries.

2. MATERIALS AND METHODS

2.1. Materials. All chemicals were purchased from commercial suppliers and used as received. Sulfuric acid (H_2SO_4) and hydrochloric acid (HCl) were supplied by Xilong Chemical Co., Ltd. Acetic acid and hydroiodic acid were purchased from Kelong Chemical Reagents Co., Ltd. Phosphoric acid (H_3PO_4) was supplied by Fuyu Fine Chemical Co., Ltd. Potassium permanganate ($KMnO_4$) and hydrogen peroxide (H_2O_2) were purchased from Tianjin Zhiyuan Chemical Reagent Co., Ltd. Graphite powder (325 mesh, 99.8%) was obtained from Alfa Aesar. Silk of *Bombyx mori* silkworm was purchased from Zhejiang Second Silk Factory. Slide-A-Lyzer Dialysis Cassette (MWCO 3500, Pierce), LiBr, poly(ethylene oxide) (PEO) with a molecular weight of 900 000, Triton X-100, ascorbic acid, 4′,6-diamidino-2-phenylindole (DAPI), FITC-phalloidin, and retinoic acid were purchased from Sigma-Aldrich. Dulbecco's modified Eagle's medium (DMEM), fetal bovine serum (FBS), and penicillin−streptomycin were purchased from Gibco. LIVE/DEAD Viability Kit, Goat Anti-Rabbit IgG H&L (Alexa Fluor 488), and Goat Anti-Mouse IgG H&L (Alexa Fluor 594) were purchased from Invitrogen (Carlsbad, CA). Anti-Nestin antibody and Anti-β3-Tubulin were purchased from Abcam.

2.2. Preparation of Graphene Oxide (GO) and Graphene Oxide Paper. We synthesized graphene oxide (GO) from natural graphite power according to an improved Hummers' method.[32] Briefly, graphite powder (3 g) was added into a mixture of concentrated H_2SO_4/H_3PO_4 (360:40 mL) and the mixture was stirred with magnetic force to make it uniform. Then, potassium permanganate (18.0 g) was slowly added into the mixture, followed by heating to 50 °C with stirring for 12 h. After cooling down to room temperature, the mixture was then poured into ice water (~400 mL) and plenty of 30% hydrogen peroxide (~3 mL) was added to terminate the reaction. Then, the reaction solution was centrifuged at 1000 rpm for 20 min to remove the excessive graphite powder. Subsequently, the graphene oxide precipitation was obtained after centrifugation at 10 000 rpm for 20 min. The remaining precipitation was washed twice with 200 mL of 30% HCl to remove metal ions and 200 mL of deionized (DI) water to remove the residual acid, and the supernatant was decanted away. Finally, the solution was purified by dialysis against DI water for 1 week to remove the remaining metal ions and obtain the graphene oxide gel. Graphene oxide paper (GOP) was obtained by casting the graphene oxide gel onto a Petri dish, followed by natural drying.[33] To obtain the reduced graphene oxide paper (rGOP) with conductivity, we immersed the GOPs in the acid solution mixed with hydroiodic acid and acetic acid (55:45 v/v) and heated the acid solution to 70 °C to reduce all of the GOPs. Then, the obtained rGOPs were washed with ethanol to remove the residual acid.[34]

2.3. Preparation of Silk Fibroin Solution. The aqueous solution of silk fibroin was prepared according to a previously reported method.[35] First, we boiled the raw silk (*B. mori*) for 20 min in 0.02 M sodium carbonate solution and rinsed it with DI water three times to remove the residual sodium carbonate. Then, 9.3 M LiBr solution was used to dissolve the dried silk fibroin at 60 °C for 4 h. After cooling down to room temperature, the solution was carefully transferred into a dialysis tube with a molecular weight cutoff of 3500 and dialyzed against Milli-Q water for 3 days to remove the remaining solvent. After dialysis, the silk fibroin was obtained by 5000 rpm centrifugation for 20 min at 5 °C. The final concentration of silk fibroin solution was determined to be 8% by calculating the remaining mass of the dried silk solid.

2.4. Electrospinning and Post-Treatment of the Mats. Silk fibroin/poly(ethylene oxide) (PEO) blended solution was prepared by mixing 8% (w/v) silk fibroin solution with 5% (w/v) PEO solution in a 4:1 volume ratio. Then, the silk/PEO solution was fed into a 10 mL syringe with a 16 G blunted stainless-steel needle and extruded at a flow rate of 1 mL/min using a customized syringe pump. The voltage between the needle and the aluminum plate was maintained at 9−10 kV. A 15 cm diameter aluminum plate was used to collect the random silk (RS) nanofibers. A high-speed rotating steel wheel was used to collect the aligned silk nanofibers. The distance between the needle and the collector was about 15 cm. Electrospinning was conducted under room temperature around 28 °C, and the environmental humidity was maintained in the range of 30−40%. To stabilize the silk fibroin nanofibers, we immersed the electrospun nanofibers in methanol for 15 min to induce a β-sheet conformational transition. Finally, PEO was scarified by immersing the samples in DI water for 72 h.[36]

2.5. Material Characterizations. The morphologies of the samples such as graphene oxide sheets, rGOP, and electrospun nanofiber−rGOP composite scaffolds were studied by a scanning electron microscope (SEM, SU-8010). The morphology of graphene oxide sheets was also characterized by atomic force microscopy (AFM, Dimension) in tapping mode. X-ray diffraction (XRD) was used to study the structure of the synthesized graphene oxide and raw graphite. The surface chemical bonds of GOP and rGOP were studied by X-ray photoelectron spectroscopy (XPS). For more quantitative analyses, we used the Gaussian components after a Shirley background subtraction to deconvolute XPS peaks. The carbon structures of the GOP and rGOP were investigated using Raman spectroscopy (inVia Reflex) with a 532 nm Nd:YAG excitation source. The electrical conductivity of the samples was evaluated by measuring the sheet resistance using four-point probe technique.

2.6. Cell Culture. The SH-SY5Y human neuroblastoma cell line, which is a well-established in vitro model for neurological studies such as neuronal differentiation and neurotoxicity, was used in this study.[37]

DOI: 10.1021/acsami.8b12562
ACS Appl. Mater. Interfaces 2018, 10, 39228−39237

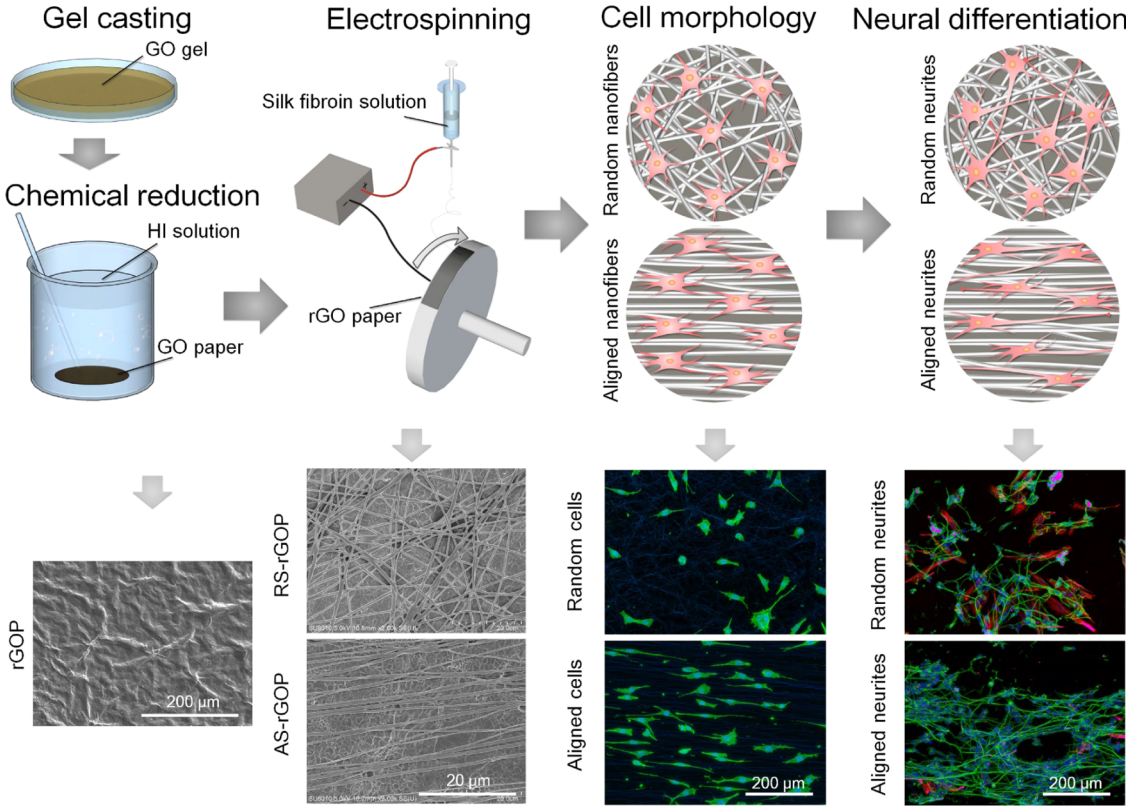

Figure 1. Schematic illustration of the fabrication of silk fibroin nanofibers on reduced graphene paper. Graphene oxide gel was cast onto a dish, followed by natural drying to obtain graphene oxide paper (GOP). Then, the GOP was transformed into a wrinkled-surface reduced graphene oxide paper (rGOP) (black disks) through hot chemical reduction in hydroiodic acid. Moreover, silk fibroin random and aligned nanofibers (white fibers) were coated on the surface of rGOP by electrospinning to obtain random silk nanofiber–rGOP (RS–rGOP) and aligned silk nanofiber–rGOP (AS–rGOP) scaffolds. Then, SH-SY5Y cells were seeded onto the scaffolds to study the cytotoxicity, proliferation, and neural differentiation.

Human neuroblastoma SH-SY5Y cells (ATCC, CRL-2266) were cultured in DMEM–nutrient mixture F12 medium supplemented with 10% fetal bovine serum (FBS), 4×10^{-3} M glutamine, 10 U mL^{-1} penicillin, and 10 mg mL^{-1} streptomycin under standard cell culture conditions (37 °C and 5% CO_2). Cells (within the 10th passage) were cultured until subconfluence.

2.7. Cytotoxicity, Proliferation, and Alignment Study. The electrospun random silk nanofiber–rGOP (RS–rGOP) and aligned silk nanofiber–rGOP (AS–rGOP) scaffolds were punched into pieces with a diameter of 10 mm and placed into a 24-well plate. Then, human neuroblastoma SH-SY5Y cells were seeded onto the rGOP and the two types of electrospun nanofiber–rGOP scaffolds at a density of 2×10^4 cells cm^{-2}. The cells were cultured in DMEM-F12 medium supplemented with 10% fetal bovine serum (FBS), 4×10^{-3} M glutamine, 10 U mL^{-1} penicillin, and 10 mg mL^{-1} streptomycin. The cell culture medium was changed every 3 days. The viability and proliferation of SH-SY5Y cells cultured on different substrates were studied using a LIVE/DEAD Viability/Cytotoxicity Assay Kit (Invitrogen), which can fluorescently label live cells with calcein-AM (green) and dead cells with ethidium homodimer-1 (red). After culturing for 1, 3, and 5 days, the samples were immersed in the calcein-AM (1/2000 PBS) and ethidium homodimer-1 (1/500 PBS) mixed staining solution for 20 min in a cell incubator. Afterward, the samples were washed three times with 1× PBS. Then, the DEAD/LIVE cells were visualized using a fluorescence microscope (Olympus IX81). The cell viability and proliferation were calculated by analyzing the DEAD/LIVE cells of five images from three different samples with NIH ImageJ Software.

For cell alignment study, after culturing for 1, 3, and 5 days, the cells were fixed with 4% paraformaldehyde for 15 min and then washed with 1× PBS three times. Next, cell membranes were permeabilized with 0.1% Triton X-100 for 15 min at room temperature and washed three times with 1× PBS to remove Triton. Then, the cells were immersed in Alexa Fluor 488 phalloidin (1:40 dilution in 1× PBS) and DAPI (1:1000 dilution in 1× PBS) for 40 min at room temperature. Afterward, the samples were washed three times with 1× PBS. Finally, the cell morphology was visualized with a laser scanning confocal microscope (Nikon A1) and the orientation of SH-SY5Y cells was quantitatively analyzed using our self-compiled Matlab program.[38]

2.8. Cell Differentiation. Cells were seeded onto the electrospun nanofiber–rGOP scaffolds, aligned silk nanofibrous scaffolds, rGOP, and tissue culture plate (TCP) at a density of 2×10^4 cells cm^{-2}. After 24 h, the cell culture medium was replaced by fresh medium supplemented with 1% FBS and 1×10^{-5} M retinoic acid (RA) to induce the neuronal differentiation of SH-SY5Y cells for 10 days. In parallel, cells cultured on aligned nanofiber–rGOP scaffolds in standard medium for 7 days were used as a control. The cultured cells were replenished with fresh medium (with or without RA) every 2 days.

2.9. Immunostaining Study. After differentiation for 10 days, SH-SY5Y cells were fixed with 4% paraformaldehyde for 15 min and then washed with 1× PBS three times. Next, cellular membranes were permeabilized with 0.1% Triton X-100 for 15 min at room temperature and washed three times with 1× PBS to remove the permeabilization solution. Then, samples were blocked in 1% bovine serum albumin (BSA) diluted in 1× PBS for 1 h at 37 °C to saturate the specific binding sites. Then, the SH-SY5Y cells with different treatments were stained with Nestin and β3-Tubulin primary antibodies. The primary antibody was diluted 500 times using 1% BSA and then added into the samples with further culturing at 4 °C overnight. Afterward, the samples were washed with 1% BSA three times and treated with a secondary antibody that was diluted 200 times in 1% BSA at 37 °C for 45 min. Then, the other protein was

DOI: 10.1021/acsami.8b12562
ACS Appl. Mater. Interfaces 2018, 10, 39228–39237

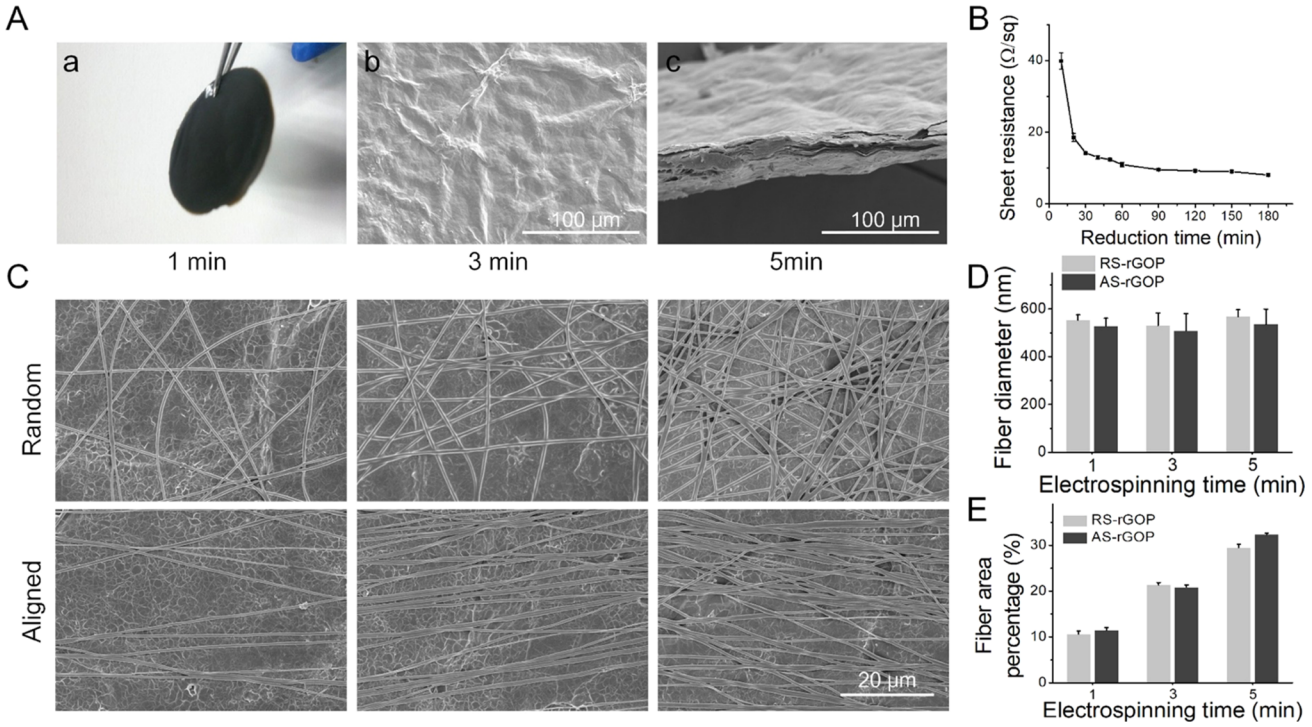

Figure 2. Characterization of materials. (A) (a) Photograph of GOP, and field emission scanning electron microscope (FE-SEM) images showing the (b) top view and (c) section view of rGOP. (B) Reduced time-dependent sheet resistance of reduced graphene oxide. (C) FE-SEM of random silk nanofibers (RS) on rGOP (RS−rGOP) by electrospinning silk fibroin for 1 min, 3 min, and 5 min, and FE-SEM of aligned silk nanofibers (AS) on rGOP (AS−rGOP) by electrospinning silk fibroin for 1 min, 3 min, and 5 min. (D) Average diameter of silk fibroin nanofibers in different electrospinning times and different electrospinning modes. (E) Silk fibroin nanofibers' area percentage in different electrospinning times and different electrospinning modes.

stained following the same protocol. Finally, the samples were stained with DAPI (1:1000 in 1× PBS) for 10 min at room temperature. After three rinses with 1× PBS, the samples were mounted and observed under a Nikon A1 laser scanning confocal microscope. The average neurite length of differentiated SH-SY5Y cells was quantified from the confocal images in Figure 5 using neurite trace plugin of NIH ImageJ Software.

2.10. Statistical Analysis. All of the experiments were repeated at least three times independently for each reported dataset (unless stated), and all showed consistent results. Data were reported as single datasets, and average values ± standard deviations (means ± SD) were used for presenting results. Data were statistically analyzed using Origin commercial software. For nonparametric data (after Shapiro−Wilk normality test), Mann−Whitney *t*-test (two-tailed) analysis was used. Statistical significance refers to results where $p < 0.05$ was obtained.

3. RESULTS AND DISCUSSION

Electroactive biomaterials hold great promise for engineering neural tissues.[39] However, the preparation of a scaffold with good electrical conductivity, biocompatibility, and micro/nanostructure has always been a great challenge.[40] Among various conductive scaffolds, rGOP has shown great potential for neural tissue regeneration because of its excellent conductivity and biocompatibility, and the ability to enhance the differentiation of stem cells.[6,11,29,41] Here, we developed a heterostructured composite scaffold composed of aligned electrospinning silk nanofibers coated on conductive rGOP to provide both electrical cue and topographic guidance for enhanced neuronal differentiation, neurite alignment, and network formation.

3.1. Fabrication and Characterizations of Nanofiber−rGOP Scaffolds. To fabricate a highly conductive and biocompatible scaffold, we cast graphene oxide gel onto a dish, followed by natural drying to obtain GOP.[33] Then, GOP was transformed into rGOP through hot chemical reduction in hydroiodic acid. Next, silk nanofibers were electrospun onto the surface of the rGOP to build two different heterogenous silk nanofiber−rGOP composite scaffolds, i.e., random silk nanofibers on GOP (termed as RS−rGOP) and aligned silk nanofibers on rGOP (termed as AS−rGOP). Finally, SH-SY5Y cells were seeded onto the scaffolds to investigate the cellular behaviors including cell viability, proliferation, morphology, and differentiation (Figure 1).

We first examined the structure of the synthesized GO using AFM and observed that the synthesized GO sheet shows a lamellar morphology (Figure S1). The GO sheet is about 5−10 μm in size (Figure S1A) and 1.2 nm in thickness (Figure S1B), confirming the successful synthesis of the GO sheet. We also observed from the TEM image that the thin layer of GO is almost transparent (Figure S1C) and has a wrinkled structure, which is probably caused by the presence of oxygen-containing functional groups of GO. Furthermore, we examined the crystal structure of GO using XRD (Figure S1D). We observed that the characteristic peak 2θ of GO is 9.8° corresponding to the (022) reflection of stacked GO sheets with a *d*-spacing of 0.92 nm. The *d*-spacing of GO is obviously lager than the *d*-spacing of pristine graphite (0.34 nm) with a characteristic peak 2θ at 26.4°, suggesting the presence of functional groups on the GO sheet surface. The image taken by a camera reveals a uniform surface morphology (Figure 2A-a). We examined the microstructure of rGOP using SEM and observed that the

DOI: 10.1021/acsami.8b12562
ACS Appl. Mater. Interfaces 2018, 10, 39228−39237

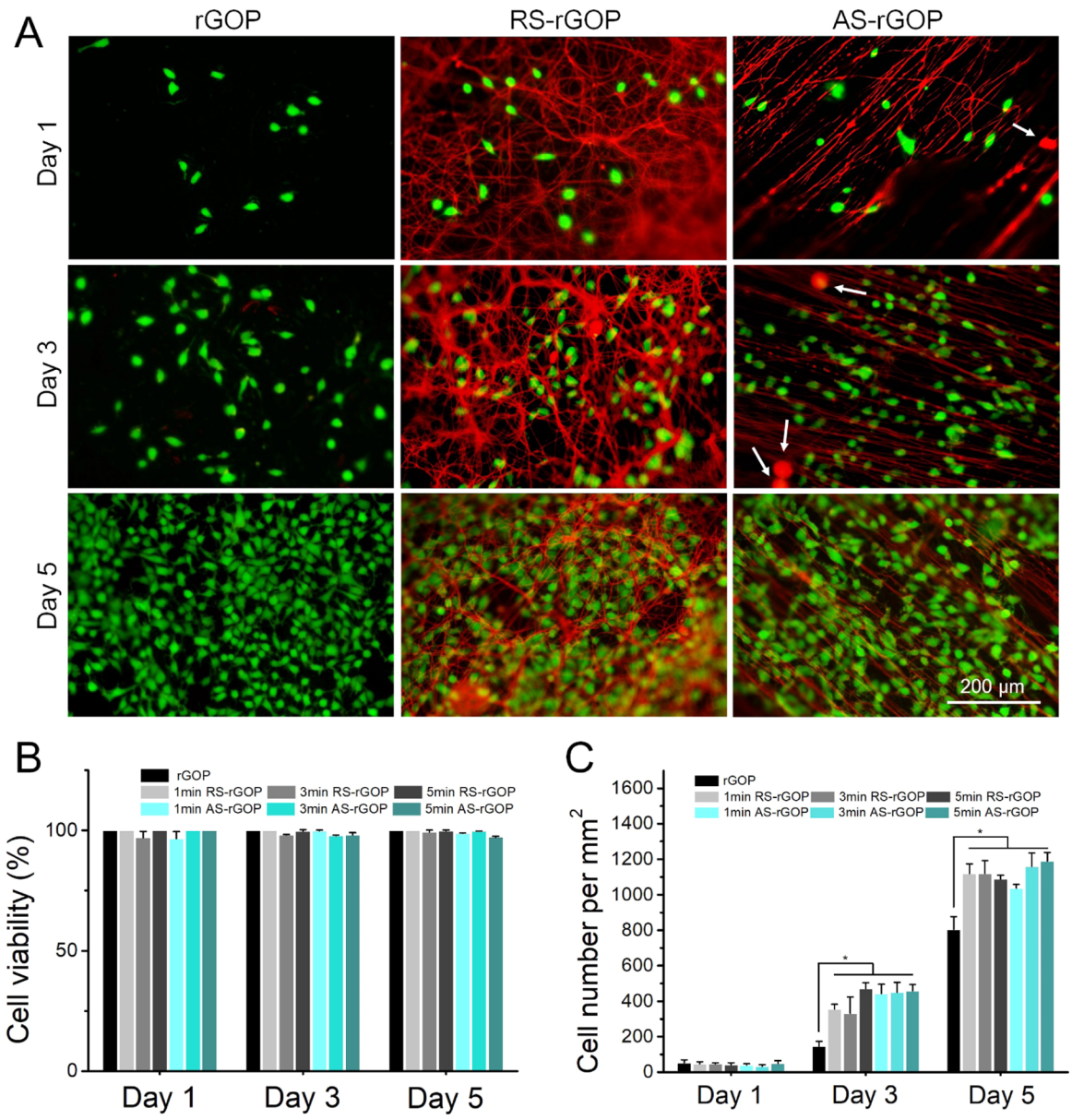

Figure 3. Viability and proliferation of SH-SY5Y cells on composite materials. (A) LIVE/DEAD fluorescent images of SH-SY5Y cells cultured on reduced graphene paper (rGOP), random silk nanofibers-rGOP (RS−rGOP) scaffold, and aligned silk nanofibers-rGOP (AS−rGOP) scaffold. The dead cells stained with red color are pointed by the white arrows. (B) Cell viability of SH-SY5Y cells cultured in each group. (C) Cell proliferation of SH-SY5Y cells cultured in each group (*$p < 0.05$).

surface of rGOP is a little wrinkled and the thickness is about 40−60 μm (Figure 2A-b,c).

To further ensure the successful synthesis of rGOP, we evaluated the chemical structure of the synthesized GOP and rGOP using Raman spectroscopy, infrared spectroscopy, and XPS (Figure S2). We observed two relatively blunt peaks of GOP at 1355.2 and 1607.3 cm^{-1} (corresponding to the D and G bands, respectively) from Raman spectroscopy, while the two peaks of rGOP appearing at the same positions become obviously sharp, demonstrating the improved degree of crystallization for rGOP as compared with GOP (Figure S2A). We further identified the chemical bonds and functional groups of GOP and rGOP using infrared spectroscopy (Figure S2B). We observed peaks of GOP at 3193 cm^{-1} referring to O−H stretching vibration, at 1736 and 1618 cm^{-1} referring to C═O stretching vibration, and at 1049 cm^{-1} referring to C−O stretching vibration. However, the above-mentioned characteristic peaks almost disappear after chemical reduction, confirming the successful synthesis of rGOP. To further reveal the deoxygenation of GOPs during reduction, we performed XPS investigations. The C 1s peak of GOP is deconvoluted into four peaks located at 284.6 eV (sp^2 carbon, C═C−C bonds), 286.7 eV (C−O bonds), 288.3 eV (C═O bonds), and 289.7 eV (O−C═O bonds) (Figure S2C). Among these, C−O bonds have the highest intensity, indicating the considerable degree of oxidation in GOP. In comparison, the oxygen-containing functional groups in terms of C−O, C═O, and O−C═O of rGOP are greatly reduced, indicating the feasibility in synthesizing rGOP through chemical reduction. The synthesized rGOP has also been proved by comparing the sheet resistance with that of GOP (Figure S2D), where the sheet resistance is remarkably reduced from ∼10 MΩ/sq of GOP to

DOI: 10.1021/acsami.8b12562
ACS Appl. Mater. Interfaces 2018, 10, 39228−39237

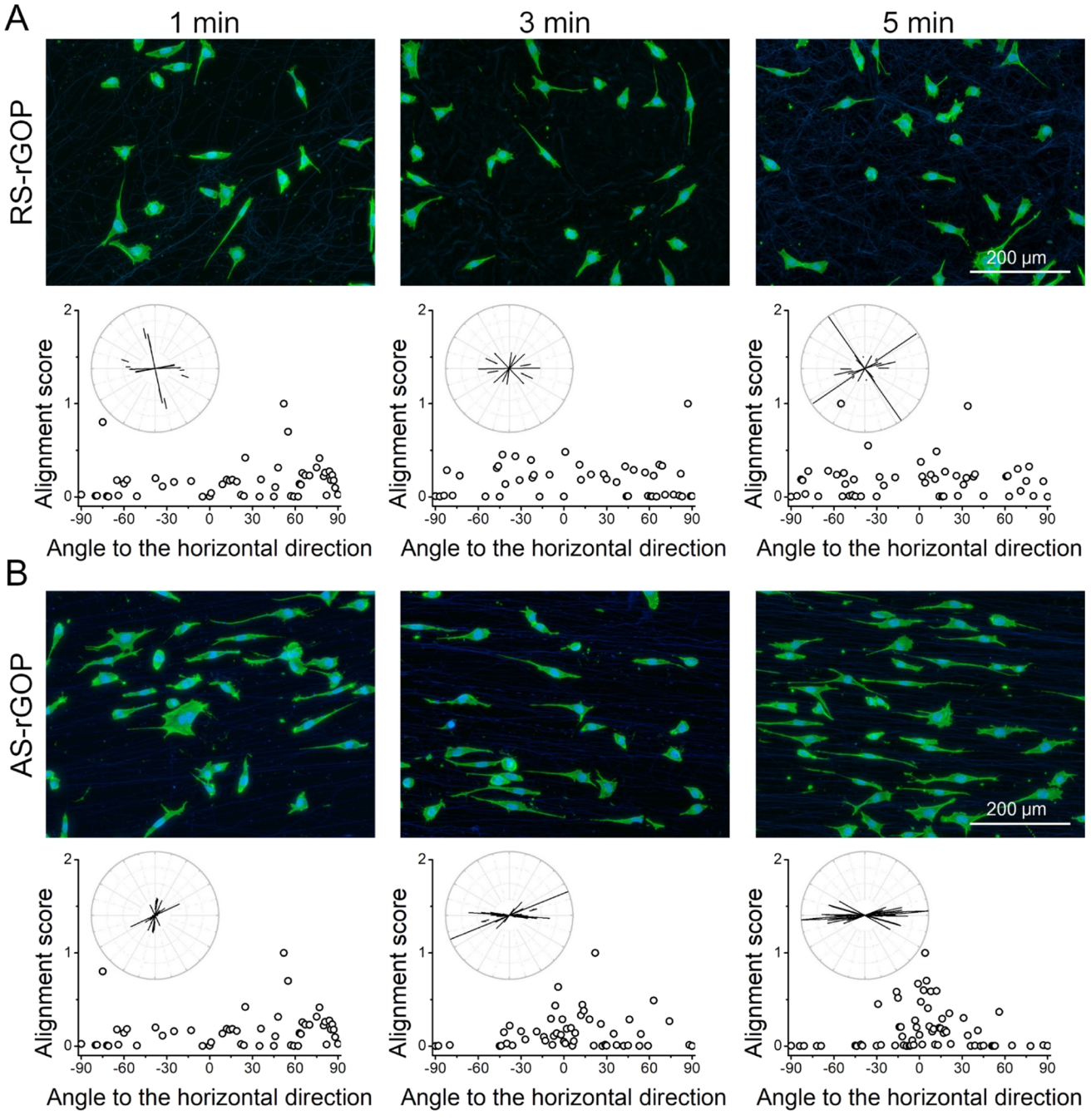

Figure 4. Cell morphology of SH-SY5Y cells. (A) Cell morphology of SH-SY5Y cells on random silk nanofiber−rGOP by electrospinning silk fibroin for 1, 3, and 5 min, and corresponding alignment scores for 1, 3, and 5 min, respectively. (B) Cell morphology of SH-SY5Y cells on aligned silk nanofiber−rGOP by electrospinning silk fibroin for 1, 3, and 5 min, and corresponding alignment scores for 1, 3, and 5 min, respectively. Phalloidin stains cell filaments green, and DAPI stains cell nuclei blue.

about ∼10 Ω/sq of rGOP (Figure 2B). The value of the sheet resistance of the samples stabilizes at ∼10 Ω/sq when the reduction time increases to 60 min. We did not observe significant changes in sheet resistance with further increase of reduction time from 60 to 180 min. Collectively, these results confirm the successful synthesis of rGOP with high conductivity.

Nanofibrous scaffolds have been intensively used for regulating stem cell fate because of their capability in mimicking the fibrous structure of native ECM.[42,43] To endow the rGOP with nanofibrous topography, we then electrospun random and aligned silk nanofibers onto rGOP to form RS−rGOP scaffold (Figure 2C random) and AS−rGOP scaffold (Figure 2C aligned), respectively. The diameter of silk nanofibers is 400−600 nm, as observed from SEM images (Figure 2D). The density of nanofibers of each sample is adjusted by changing electrospinning duration in terms of average nanofibers' area percentages, which are about 10, 20, and 30% through 1, 3, and 5 min electrospinning, respectively (Figure 2E). Since the rGOP surface is not fully covered by nanofibers, it can directly contact with the attached SH-SY5Y cells providing electric activities. The obtained nanofibers and rGOP composite scaffolds with a uniform fiber diameter and

DOI: 10.1021/acsami.8b12562
ACS Appl. Mater. Interfaces 2018, 10, 39228−39237

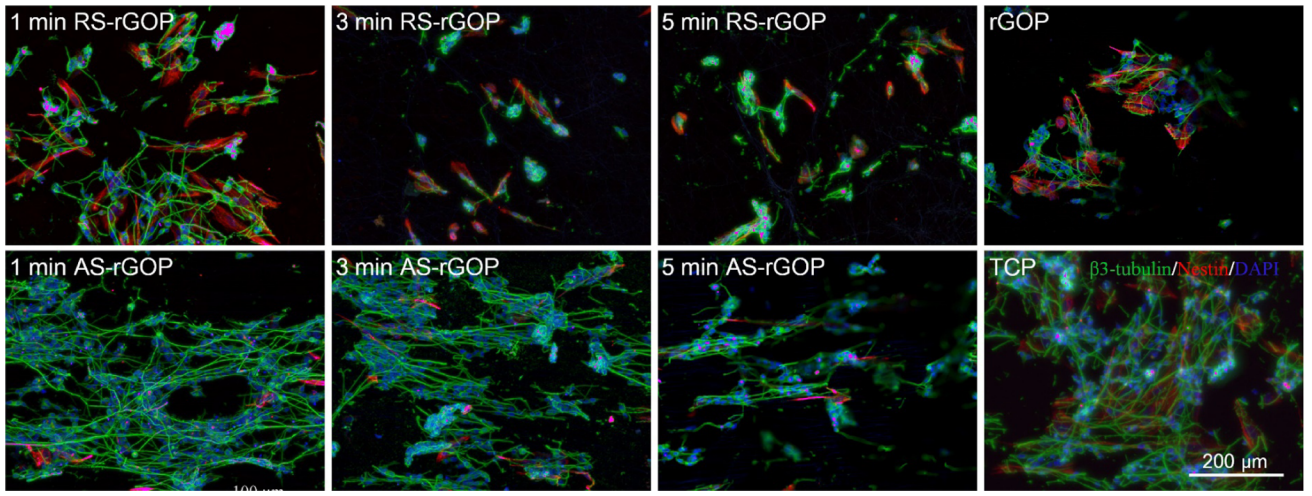

Figure 5. Confocal images of SH-SY5Y cell differentiation on the composite scaffold. The upper row shows the differentiated SH-SY5Y cells attached on random silk nanofiber−rGOP by electrospinning silk fibroin for 1, 3, and 5 min, as well as on rGOP. The lower row shows the differentiated SH-SY5Y cells attached on aligned silk nanofiber−rGOP by electrospinning silk fibroin for 1, 3, and 5 min, as well as on TCP. High expression of neuron-specific marker β3-tubulin (green color) was found on the aligned silk (AS) nanofibers collected on rGOP by electrospinning for 1 min as compared to the cells attached on other substrates. The neural stem cell specific marker Nestin was revealed in red color.

homogeneous fiber distribution hold great potential for guiding stem cell fate in the following experiments.

3.2. Cytotoxicity of the Nanofiber−rGOP Scaffolds. To assess the cytotoxicity of the heterogeneous composite scaffolds, we seeded SH-SY5Y cells onto three different scaffolds (i.e., the rGOP group, RS−rGOP group, and AS−rGOP group) and monitored the cell viability and proliferation (Figure 3). We observed that the SH-SY5Y cells can adhere to all three scaffolds (Figure S4). Most cells remain alive, as indicated by the LIVE/DEAD staining assay (Figure 3A), which is further confirmed by the quantification results that cell viability remains as high as 95% in all of the samples throughout the experiment (Figure 3B). Cells are able to proliferate on three scaffolds over 5 days, but cell proliferation on RS−rGOP and AS−rGOP scaffolds is significantly higher than that of cells on rGOP scaffold (Figure 3C), confirming the improved biocompatibility of composite scaffolds after silk nanofiber deposition.

3.3. Guidance of Cell Alignment on the Nanofiber−rGOP Scaffolds. Topographical cues of biomaterials have been proved to have a significant role in regulating stem cell behaviors such as cell adhesion, proliferation, self-renewal, gene expression, morphology, and differentiation.[15,44] Especially, inspired by the highly oriented features of native ECMs in nerve tissues, aligned nanofibrous scaffolds have been widely used as topographical cues in controlling the functions of stem cells.[45] To study the guiding effects of nanofiber−rGOP scaffolds, we stained the SH-SY5Y cells cultured for 1 day on RS−rGOP and AS−rGOP scaffolds with different nanofiber densities (Figure 4). Then, we quantified the orientation of cells in directions ranging from −90 to 90°. We observed that the SH-SY5Y cells are randomly grown on all of the three RS−rGOP scaffolds, as clearly illustrated in Figure 4A.

However, the SH-SY5Y cells cultured on the AS−rGOP scaffolds have apparently different cell morphologies and alignments from the cells on the RS−rGOP scaffolds (Figure 4B). The SH-SY5Y cells on all of the three AS−rGOP scaffolds show a clear oriented growth, and the cell alignment is enhanced with increasing nanofiber density. The cells possess a dominant axis in directions around 0°, indicating that the cell arrangement on AS−rGOP scaffolds is highly aligned (Figure 4B). With the prolonged cell culture duration for 3 days, the cells on AS−rGOP scaffolds show significantly improved alignment as compared with the cells cultured on the RS−rGOP scaffolds (Figure S5).

3.4. Neuronal Differentiation of SH-SY5Y Cells on the Nanofiber−rGOP Scaffolds. Inspired by the promising cell proliferation and arrangement results, we examined the capability of nanofiber−rGOP scaffolds in guiding the neuronal differentiation of SH-SY5Y cells. We observed the formation of elongated neurites and expression of mature neuronal maker β3-Tubulin, confirming neuronal differentiation of SH-SY5Y cells (Figure 5). To further evaluate the neuronal differentiation of SH-SY5Y cells on different substrates, we quantified the average neurite length of cells on each substrate, and the results are shown in Figure S6. The average neurite length of cells on AS−rGOP scaffolds is longer than that on RS−rGOP scaffolds, revealing the superior capability of AS−rGOP scaffolds in guiding neuronal differentiation. Moreover, the SH-SY5Y cells attached to AS−rGOP scaffolds with 1 min nanofiber deposition have the longest neurite outgrowth, further confirming the strong capability of AS−rGOP scaffolds in promoting the neuronal differentiation of SH-SY5Y cells (Figure S6). On 1 min aligned silk nanofiber−rGOP scaffolds, the SH-SY5Y cells exhibited cluster growth and formed longer oriented neurites and neural networks.

With the increase of the aligned nanofiber density on the rGOP scaffold, the neurites become shorter and the density of neurites become lower. This could be attributed to the decreased area of the conductive rGOP surface that cells can attach to and sense. The SH-SY5Y cells cultured on the pure electrospun aligned silk nanofibers alone show limited expression of β3-Tubulin (Figure S7). These results confirm the important role of the conductive rGOP in regulating stem cell neuronal differentiation. As compared with cells on RS−rGOP and rGOP scaffolds (Figure 5), cells on AS−rGOP scaffolds show significantly higher expression of β3-Tubulin and longer neurite outgrowth, revealing that the topographical

DOI: 10.1021/acsami.8b12562
ACS Appl. Mater. Interfaces 2018, 10, 39228−39237

cues provided by the aligned nanofibers are as important as the conductive rGOP in guiding stem cell neuronal differentiation.

We further studied the neuronal differentiation of SH-SY5Y cells with only biophysical and topographical cues (AS−rGOP scaffold) without adding RA in the cell culture medium (Figure S8). We found that the cells proliferate continuously until the cells fully cover the surface of the materials, indicating the limited neuronal differentiation. Meanwhile, the average neurite length of cells on the AS−rGOP scaffolds with 1 and 3 min nanofiber deposition is significantly higher than that on TCP with biochemical cue (RA) stimulation (Figure S6). These results demonstrate that although biophysical and topographical cues alone show limited capability in promoting the neuronal differentiation of SH-SY5Y cells, they do enhance the differentiation when combined with a biochemical cue (RA) (Figures 5 and S6). Collectively, the designed AS−rGOP scaffold with the combination of conductive rGOP and aligned nanofibers (electrospun for 1 min) is the optimized scaffold in promoting the neuronal differentiation of SH-SY5Y cells with the oriented arrangement and neural network formation.

4. DISCUSSION

It is still a great challenge to construct electroactive scaffolds that can induce the oriented growth of nerve cells and promote the differentiation and network formation of NSCs for the regeneration of nerve tissues because of the lack of biocompatibility of most conductive materials.[6,46] Graphene materials with high electrical conductivity and good biocompatibility hold great potential in treating nerve tissue defects.[6,11] Previous studies have blended graphene or graphene oxide as addition materials into electrospinning solution to fabricate electrospun nanofibrous scaffolds. This blending method requires the fragmentation of graphene, which increases the potential toxicity and weakens the electrical properties of nanofibers.[47] Some researchers have adopted the electrospinning method to prepare the scaffolds first, followed by adsorption of a graphene sheet on the scaffold surface, but their investigation is focused on the disordered scaffolds and the electrical conductivity is still low.[29] How to design and prepare scaffolds with good electrical conductivity, biocompatibility, and directional topological nanostructure has remained a key research problem. The cast rGOP with extraordinary electrical conductivity and favorable biocompatibility has been proved to effectively enhance the neuronal differentiation of SH-SY5Y.[6,11,21,22] However, as compared with the GOP, rGOP reduces the cell adhesion ability because of the reduction of surface functional groups (e.g., hydroxyl, carboxyl, and carbonyl groups), which affects the adsorption capacity and binding ability of cell proteins. In addition, the planar rGOP cannot effectively guide the attached SH-SY5Y cell orientation, which is highly desired for forming a well-aligned cellular construct like nerve tissues.

In this work, we electrospun aligned silk nanofibers onto the surface of rGOP to fabricate a novel heterogeneous composite scaffold for guiding SH-SY5Y-cell-oriented growth and mature neuronal differentiation. SH-SY5Y human neuroblastoma cells have some characteristics of NSCs such as neuronal differential capacity.[37,48−50] Hence, the SH-SY5Y human neuroblastoma cells have been intensively used as an in vitro model for neurological studies, including neuronal differentiation and functions related to neurodegenerative processes and neurotoxicity.[37,51−53] Therefore, we also used SH-SY5Y human neuroblastoma cells as an in vitro model to verify our hypothesis. The composite scaffold is very stable, and the nanofibers are firmly attached to the rGOP, as demonstrated by the firm attachment without falling of nanofibers even in 1 week of solution perturbation. The arrangement and density of nanofibers can be adjusted by choosing the design of the nanofiber collector (plate collector or a rolling wheel) and the nanofiber deposition duration (Figure 2). The synthesized AS−rGOP scaffold has excellent conductivity, biocompatibility, and aligned topographical cue that can mimic the native ECM of a nerve tissue. Therefore, the composite scaffold could improve the electrotransport performance of the cells and also successfully promote the cell adhesion and proliferation, and induce the cells to grow directionally (Figure 3). We have found that the cell alignment is strongly dependent on the nanofiber density and orientation, where cell alignment is significantly enhanced with increasing nanofiber density and fiber alignment (Figure 4). This may favor cell growth along the fiber direction and cell−cell connection to form a network structure, which is of great significance for the regeneration of a functional nerve tissue. The cell differentiation results show that our nanofiber−graphene composite scaffolds can not only induce the neuronal differentiated SH-SY5Y cell neurites to arrange along the fiber direction but also promote the maturity of SH-SY5Y cells with significant expression of neuronal maker β3-Tubulin. It should be noted that the AS−rGOP scaffold (1 min) with the highest available area of conductive rGOP for cell sensing showed the strongest capability in promoting the neuronal differentiation of SH-SY5Y cells, confirming the robust role of rGOP in regulating stem cell neuronal differentiation. In summary, we have fabricated oriented nanofiber−graphene heterogeneous composite scaffolds, which have the advantages of simple preparation process and controllable parameters. Additionally, the AS−rGOP scaffold can promote the alignment and neuronal differentiation of SH-SY5Y cells. Our design method of such composite scaffolds provides an inspiration for the surface modification of bioscaffolds.

5. CONCLUSIONS

In this study, we designed and fabricated a new heterostructure composite scaffold composed of aligned electrospinning silk fibroin nanofibers and conductive rGOP, which exhibited excellent conductivity and biocompatibility. This heterogeneous composite scaffold with 10% area of nanofibers coated on the conductive rGOP can effectively induce the oriented growth of SH-SY5Y cells, enhancement of SH-SY5Y cells neuronal differentiation, and formation of neural networks. This work provides a pioneered design of a graphene nanosheet and silk nanofibers hybrid scaffold for controlling the differentiation of NSCs and axon orientation, which holds great potential for effective stem cell therapy of neurological diseases and injuries.

■ ASSOCIATED CONTENT

Supporting Information

The Supporting Information is available free of charge on the ACS Publications website at DOI: 10.1021/acsami.8b12562.

Characterizations of graphene oxide, GOP and rGOP; LIVE/DEAD fluorescent images of SH-SY5Y cells; cell morphology of SH-SY5Y cells; average neurite length of differentiated SH-SY5Y cells, and confocal images of SH-

DOI: 10.1021/acsami.8b12562
ACS Appl. Mater. Interfaces 2018, 10, 39228−39237

SY5Y cell differentiation on aligned silk nanofibers (PDF)

AUTHOR INFORMATION

Corresponding Authors

*E-mail: tjlu@nuaa.edu.cn (T.J.L.).
*E-mail: fengxu@mail.xjtu.edu.cn (F.X.).

ORCID

Zhengtang Luo: 0000-0002-4822-9694
Feng Xu: 0000-0003-4351-0222

Author Contributions

○H.Q. and G.J. contributed equally to this work.

Notes

The authors declare no competing financial interest.

ACKNOWLEDGMENTS

This research was supported by the National Natural Science Foundation of China (11522219, 31600804, 11761161004, and 11532009), the International Science & Technology Cooperation Program of China (2013DFG02930), Natural Science Basic Research Plan in Shaanxi Province of China (2017JM8097 and 2017JQ3035), and National Project Cultivating Foundation of Xi'an Medical University (2017GJFY23).

REFERENCES

(1) Thompson, D. M.; Koppes, A. N.; Hardy, J. G.; Schmidt, C. E. Electrical Stimuli in the Central Nervous System Microenvironment. *Annu. Rev. Biomed. Eng.* **2014**, *16*, 397−430.

(2) Pires, A. O.; Neves-Carvalho, A.; Sousa, N.; Salgado, A. J. The Secretome of Bone Marrow and Wharton Jelly Derived Mesenchymal Stem Cells Induces Differentiation and Neurite Outgrowth in SH-SY5Y Cells. *Stem Cells Int.* **2014**, No. 438352.

(3) Achilleos, A.; Trainor, P. A. Neural crest stem cells: discovery, properties and potential for therapy. *Cell Res.* **2012**, *22*, 288−304.

(4) Choi, S. S.; An, J.; Lee, H. J.; Kim, S. U. Cell Therapy of Human Neural Stem Cells Overexpressing Glial Cell Line-Derived Neurotrophic Factor in Spinal Cord Injured Rat. *Cell Transplant.* **2013**, *22*, 898.

(5) Fabbro, A.; Scaini, D.; Leon, V.; Vazquez, E.; Cellot, G.; Privitera, G.; Lombardi, L.; Torrisi, F.; Tomarchio, F.; Bonaccorso, F.; Bosi, S.; Ferrari, A. C.; Ballerini, L.; Prato, M. Graphene-Based Interfaces Do Not Alter Target Nerve Cells. *ACS Nano* **2016**, *10*, 615−623.

(6) Solanki, A.; Chueng, S. T. D.; Yin, P. T.; Kappera, R.; Chhowalla, M.; Lee, K. B. Axonal alignment and enhanced neuronal differentiation of neural stem cells on graphene-nanoparticle hybrid structures. *Adv. Mater.* **2013**, *25*, 5477−5482.

(7) Thompson, B. C.; Murray, E.; Wallace, G. G. Graphite Oxide to Graphene. Biomaterials to Bionics. *Adv. Mater.* **2015**, *27*, 7563−7582.

(8) Zhang, X.; Cai, J.; Klueber, K. M.; Guo, Z. F.; Lu, C. L.; Winstead, W. I.; Qiu, M. S.; Roisen, F. J. Role of transcription factors in motoneuron differentiation of adult human olfactory neuroepithelial-derived progenitors. *Stem Cells* **2006**, *24*, 434−442.

(9) Mothe, A. J.; Tam, R. Y.; Zahir, T.; Tator, C. H.; Shoichet, M. S. Repair of the injured spinal cord by transplantation of neural stem cells in a hyaluronan-based hydrogel. *Biomaterials* **2013**, *34*, 3775−3783.

(10) Ning, Y.; Huang, J.; Kalionis, B.; Bian, Q.; Dong, J.; Wu, J.; Tai, X.; Xia, S.; Shen, Z. Oleanolic Acid Induces Differentiation of Neural Stem Cells to Neurons: An Involvement of Transcription Factor Nkx-2.5. *Stem Cells Int.* **2015**, *2015*, 1−12.

(11) Park, S. Y.; Park, J.; Sim, S. H.; Sung, M. G.; Kim, K. S.; Hong, B. H.; Hong, S. Enhanced Differentiation of Human Neural Stem Cells into Neurons on Graphene. *Adv. Mater.* **2011**, *23*, H263−H267.

(12) Guo, W.; Zhang, X. D.; Yu, X.; Wang, S.; Qiu, J. C.; Tang, W.; Li, L. L.; Liu, H.; Wang, Z. L. Self-Powered Electrical Stimulation for Enhancing Neural Differentiation of Mesenchymal Stem Cells on Graphene-Poly(3,4-ethylenedioxythiophene) Hybrid Microfibers. *ACS Nano* **2016**, *10*, 5086−5095.

(13) Niu, X. F.; Rouabhia, M.; Chiffot, N.; King, M. W.; Zhang, Z. An electrically conductive 3D scaffold based on a nonwoven web of poly(l-lactic acid) and conductive poly(3,4-ethylenedioxythiophene). *J. Biomed. Mater. Res., Part A* **2015**, *103*, 2635−2644.

(14) Guo, W.; Zhang, X.; Yu, X.; Wang, S.; Qiu, J.; Tang, W.; Li, L.; Liu, H.; Wang, Z. L. Self-Powered Electrical Stimulation for Enhancing Neural Differentiation of Mesenchymal Stem Cells on Graphene-Poly(3,4-ethylenedioxythiophene) Hybrid Microfibers. *ACS Nano* **2016**, *10*, 5086−5095.

(15) Dalby, M. J.; Gadegaard, N.; Oreffo, R. O. C. Harnessing nanotopography and integrin-matrix interactions to influence stem cell fate. *Nat. Mater.* **2014**, *13*, 558−569.

(16) Celiz, A. D.; Smith, J. G. W.; Langer, R.; Anderson, D. G.; Winkler, D. A.; Barrett, D. A.; Davies, M. C.; Young, L. E.; Denning, C.; Alexander, M. R. Materials for stem cell factories of the future. *Nat. Mater.* **2014**, *13*, 570−579.

(17) Forciniti, L.; Ybarra, J.; Zaman, M. H.; Schmidt, C. E. Schwann cell response on polypyrrole substrates upon electrical stimulation. *Acta Biomater.* **2014**, *10*, 2423−2433.

(18) Li, M.; Guo, Y.; Wei, Y.; MacDiarmid, A. G.; Lelkes, P. I. Electrospinning polyaniline-contained gelatin nanofibers for tissue engineering applications. *Biomaterials* **2006**, *27*, 2705−2715.

(19) Li, X.; Zhang, G. Y.; Bai, X. D.; Sun, X. M.; Wang, X. R.; Wang, E.; Dai, H. J. Highly conducting graphene sheets and Langmuir-Blodgett films. *Nat. Nanotechnol.* **2008**, *3*, 538−542.

(20) Lee, C.; Wei, X. D.; Kysar, J. W.; Hone, J. Measurement of the elastic properties and intrinsic strength of monolayer graphene. *Science* **2008**, *321*, 385−388.

(21) Bendali, A.; Hess, L. H.; Seifert, M.; Forster, V.; Stephan, A. F.; Garrido, J. A.; Picaud, S. Purified Neurons can Survive on Peptide-Free Graphene Layers. *Adv. Healthcare Mater.* **2013**, *2*, 929−933.

(22) Liu, H. W.; Huang, W. C.; Chiang, C. S.; Hu, S. H.; Liao, C. H.; Chen, Y. Y.; Chen, S. Y. Arrayed rGOSH/PMASH Microcapsule Platform Integrating Surface Topography, Chemical Cues, and Electrical Stimulation for Three-Dimensional Neuron-Like Cell Growth and Neurite Sprouting. *Adv. Funct. Mater.* **2014**, *24*, 3715−3724.

(23) Weaver, C. L.; Cui, X. T. Directed Neural Stem Cell Differentiation with a Functionalized Graphene Oxide Nanocomposite. *Adv. Healthcare Mater.* **2015**, *4*, 1408−1416.

(24) Shao, W.; He, J. X.; Sang, F.; Ding, B.; Chen, L.; Cui, S. Z.; Li, K. J.; Han, Q. M.; Tan, W. L. Coaxial electrospun aligned tussah silk fibroin nanostructured fiber scaffolds embedded with hydroxyapatite-tussah silk fibroin nanoparticles for bone tissue engineering. *Mater. Sci. Eng., C* **2016**, *58*, 342−351.

(25) Gnavi, S.; Fornasari, B. E.; Tonda-Turo, C.; Laurano, R.; Zanetti, M.; Ciardelli, G.; Geuna, S. The Effect of Electrospun Gelatin Fibers Alignment on Schwann Cell and Axon Behavior and Organization in the Perspective of Artificial Nerve Design. *Int. J. Mol. Sci.* **2015**, *16*, 12925−12942.

(26) Lee, B. K.; Ju, Y. M.; Cho, J. G.; Jackson, J. D.; Lee, S. J.; Atala, A.; Yoo, J. J. End-to-side neurorrhaphy using an electrospun PCL/collagen nerve conduit for complex peripheral motor nerve regeneration. *Biomaterials* **2012**, *33*, 9027−9036.

(27) Hu, K.; Gupta, M. K.; Kulkarni, D. D.; Tsukruk, V. V. Ultra-Robust Graphene Oxide-Silk Fibroin Nanocomposite Membranes. *Adv. Mater.* **2013**, *25*, 2301−2307.

(28) Baker, B. M.; Trappmann, B.; Wang, W. Y.; Sakar, M. S.; Kim, I. L.; Shenoy, V. B.; Burdick, J. A.; Chen, C. S. Cell-mediated fibre recruitment drives extracellular matrix mechanosensing in engineered fibrillar microenvironments. *Nat. Mater.* **2015**, *14*, 1262−1268.

(29) Shah, S.; Yin, P. T.; Uehara, T. M.; Chueng, S. T. D.; Yang, L. T.; Lee, K. B. Guiding Stem Cell Differentiation into Oligoden-

DOI: 10.1021/acsami.8b12562
ACS Appl. Mater. Interfaces 2018, 10, 39228−39237

drocytes Using Graphene-Nanofiber Hybrid Scaffolds. *Adv. Mater.* **2014**, *26*, 3673−3680.
(30) Qu, J.; Wang, D.; Wang, H.; Dong, Y.; Zhang, F.; Zuo, B.; Zhang, H. Electrospun silk fibroin nanofibers in different diameters support neurite outgrowth and promote astrocyte migration. *J. Biomed. Mater. Res., Part A* **2013**, *101*, 2667−2678.
(31) Chew, S. Y.; Mi, R. F.; Hoke, A.; Leong, K. W. Aligned protein-polymer composite fibers enhance nerve regeneration: A potential tissue-engineering platform. *Adv. Funct. Mater.* **2007**, *17*, 1288−1296.
(32) Marcano, D. C.; Kosynkin, D. V.; Berlin, J. M.; Sinitskii, A.; Sun, Z. Z.; Slesarev, A.; Alemany, L. B.; Lu, W.; Tour, J. M. Improved Synthesis of Graphene Oxide. *ACS Nano* **2010**, *4*, 4806−4814.
(33) Xiong, Z.; Liao, C. L.; Han, W. H.; Wang, X. G. Mechanically Tough Large-Area Hierarchical Porous Graphene Films for High-Performance Flexible Supercapacitor Applications. *Adv. Mater.* **2015**, *27*, 4469−4475.
(34) Pei, S. F.; Cheng, H. M. The reduction of graphene oxide. *Carbon* **2012**, *50*, 3210−3228.
(35) Rockwood, D. N.; Preda, R. C.; Yucel, T.; Wang, X. Q.; Lovett, M. L.; Kaplan, D. L. Materials fabrication from *B. mori* silk fibroin. *Nat. Protoc.* **2011**, *6*, 1612−1631.
(36) Zhang, X.; Baughman, C. B.; Kaplan, D. L. In vitro evaluation of electrospun silk fibroin scaffolds for vascular cell growth. *Biomaterials* **2008**, *29*, 2217−2227.
(37) Tonazzini, I.; Cecchini, A.; Elgersma, Y.; Cecchini, M. Interaction of SH-SY5Y Cells with Nanogratings During Neuronal Differentiation: Comparison with Primary Neurons. *Adv. Healthcare Mater.* **2014**, *3*, 581−587.
(38) Xu, F.; Beyazoglu, T.; Hefner, E.; Gurkan, U. A.; Demirci, U. Automated and Adaptable Quantification of Cellular Alignment from Microscopic Images for Tissue Engineering Applications. *Tissue Eng., Part C* **2011**, *17*, 641−649.
(39) Manchineella, S.; Thrivikraman, G.; Khanum, K. K.; Ramamurthy, P. C.; Basu, B.; Govindaraju, T. Pigmented Silk Nanofibrous Composite for Skeletal Muscle Tissue Engineering. *Adv. Healthcare Mater.* **2016**, *5*, 1222−1232.
(40) Mehrali, M.; Thakur, A.; Pennisi, C. P.; Talebian, S.; Arpanaei, A.; Nikkhah, M.; Dolatshahi-Pirouz, A. Nanoreinforced Hydrogels for Tissue Engineering: Biomaterials that are Compatible with Load-Bearing and Electroactive Tissues. *Adv. Mater.* **2017**, *29*, No. 1603612.
(41) Wang, Y.; Lee, W. C.; Manga, K. K.; Ang, P. K.; Lu, J.; Liu, Y. P.; Lim, C. T.; Loh, K. P. Fluorinated graphene for promoting neuro-induction of stem cells. *Adv. Mater.* **2012**, *24*, 4285−4290.
(42) Alamein, M. A.; Liu, Q.; Stephens, S.; Skabo, S.; Warnke, F.; Bourke, R.; Heiner, P.; Warnke, P. H. Nanospiderwebs: Artificial 3D Extracellular Matrix from Nanofibers by Novel Clinical Grade Electrospinning for Stem Cell Delivery. *Adv. Healthcare Mater.* **2013**, *2*, 702−717.
(43) Li, X. R.; Liang, H.; Sun, J.; Zhuang, Y.; Xu, B.; Dai, J. W. Electrospun Collagen Fibers with Spatial Patterning of SDF1 alpha for the Guidance of Neural Stem Cells. *Adv. Healthcare Mater.* **2015**, *4*, 1869−1876.
(44) Kingham, E.; Oreffo, R. O. C. Embryonic and Induced Pluripotent Stem Cells: Understanding, Creating, and Exploiting the Nano-Niche for Regenerative Medicine. *Acs Nano* **2013**, *7*, 1867−1881.
(45) Montero, R. B.; Vial, X.; Nguyen, D. T.; Farhand, S.; Reardon, M.; Pham, S. M.; Tsechpenakis, G.; Andreopoulos, F. M. bFGF-containing electrospun gelatin scaffolds with controlled nano-architectural features for directed angiogenesis. *Acta Biomater.* **2012**, *8*, 1778−1791.
(46) Fattahi, P.; Yang, G.; Kim, G.; Abidian, M. R. A Review of Organic and Inorganic Biomaterials for Neural Interfaces. *Adv. Mater.* **2014**, *26*, 1846−1885.
(47) Song, J. Q.; Gao, H. C.; Zhu, G. L.; Cao, X. D.; Shi, X. T.; Wang, Y. J. The preparation and characterization of polycaprolactone/graphene oxide biocomposite nanofiber scaffolds and their application for directing cell behaviors. *Carbon* **2015**, *95*, 1039−1050.
(48) Buttiglione, M.; Vitiello, F.; Sardella, E.; Petrone, L.; Nardulli, M.; Favia, P.; d'Agostino, R.; Gristina, R. Behaviour of SH-SY5Y neuroblastoma cell line grown in different media and on different chemically modified substrates. *Biomaterials* **2007**, *28*, 2932−2945.
(49) Genchi, G. G.; Ceseracciu, L.; Marino, A.; Labardi, M.; Marras, S.; Pignatelli, F.; Bruschini, L.; Mattoli, V.; Ciofani, G. P(VDF-TrFE)/BaTiO3 Nanoparticle Composite Films Mediate Piezoelectric Stimulation and Promote Differentiation of SH-SY5Y Neuroblastoma Cells. *Adv. Healthcare Mater.* **2016**, *5*, 1808−1820.
(50) Marino, A.; Ciofani, G.; Filippeschi, C.; Pellegrino, M.; Pellegrini, M.; Orsini, P.; Pasqualetti, M.; Mattoli, V.; Mazzolai, B. Two-photon polymerization of sub-micrometric patterned surfaces: Investigation of cell-substrate interactions and improved differentiation of neuron-like cells. *ACS Appl. Mater. Interfaces* **2013**, *5*, 13012−13021.
(51) Shipley, M. M.; Mangold, C. A.; Szpara, M. L. Differentiation of the SH-SY5Y Human Neuroblastoma Cell Line. *J. Visualized Exp.* **2016**, No. 53193.
(52) Dai, H.; Deng, Y. Y.; Zhang, J.; Han, H. L.; Zhao, M. Y.; Li, Y.; Zhang, C.; Tian, J.; Bing, G. Y.; Zhao, L. L. PINK1/Parkin-mediated mitophagy alleviates chlorpyrifos-induced apoptosis in SH-SY5Y cells. *Toxicology* **2015**, *334*, 72−80.
(53) Filograna, R.; Civiero, L.; Ferrari, V.; Codolo, G.; Greggio, E.; Bubacco, L.; Beltramini, M.; Bisaglia, M. Analysis of the Catecholaminergic Phenotype in Human SH-SY5Y and BE(2)-M17 Neuroblastoma Cell Lines upon Differentiation. *PLoS One* **2015**, *10*, No. e0136769.

DOI: 10.1021/acsami.8b12562
ACS Appl. Mater. Interfaces 2018, 10, 39228−39237